SLAB EFFECTS IN SMRF RETROFIT CONNECTION TESTS

by

Scott A. Civjan
Department of Civil and Environment Engeering
University of Massachusetts
Amherst, MA 01003-5205, USA
and
Michael D. Engelhardt
Department of Civil Engeering
Phil M. Ferguson Struct. Engrg. Lab.
Univ. of Texas
Austin, TX 78758, USA
and
John L. Gross
Building and Fire Research Laboratory
National Institute of Standards and Technology
Gaithersburg, MD 20899-8611, USA

Reprinted from the Journal of Structural Engineering, Vol. 127, No. 3, 230-237, March 2001.

NOTE: This paper is a contribution of the National Institute of Standards and Technology and is not subject to copyright.

NIST
National Institute of Standards and Technology
Technology Administration, U.S. Department of Commerce

SLAB EFFECTS IN SMRF RETROFIT CONNECTION TESTS

By Scott A. Civjan,[1] P.E., Michael D. Engelhardt,[2] P.E., and John L. Gross,[3] P.E., Members, ASCE

ABSTRACT: A series of six full-scale subassemblages were tested to investigate dogbone and haunch retrofits for pre-Northridge steel moment connections. Tests included matched pairs of specimens, one bare steel and one including composite slab. Data were collected to evaluate the influence and behavior of the concrete slab. Results that emphasize the influence of the composite slab on connection behavior and specific comments on the slab response are presented. The presence of a composite slab corresponded to higher-achieved overall plastic rotations and higher-peak attained moments. Existing estimates of composite beam capacity overestimated the specimen strengths in positive moment. Shear stud failures were observed, raising concerns about the capacity of shear studs under severe reversed cyclic loading.

INTRODUCTION

The 1994 Northridge Earthquake caused extensive, and largely unexpected, damage in steel moment resisting frames (SMRFs) (SAC 1995; Youssef et al. 1995). A research project was conducted to investigate possible retrofit methods for pre-Northride SMRF connections. This project tested six full-scale subassemblages under quasi-static, reversed cyclic loading. Three of these specimens included a composite slab. Overall results and specimen details were reported in Civjan et al. (2000). This paper focuses on the behavior and influence of the composite slabs in this study.

The effects of composite slabs on SMRF connection behavior, under reversed cyclic loads, has received only limited attention in past research. Most testing has included fully composite slabs with significant amounts of slab reinforcement that may not be representative of many existing buildings. Du Plessis and Daniels (1972) found that the slab contribution under cycled positive moments (slab in compression) was related to a compression zone that acts over the width of the column face and the depth of the slab in contact with the column face. The compressive stress acting at this location was reported as $1.3f'_c$. Lee and Lu (1989) tested a specimen under reversed cyclic moments and reported peak strengths less than that predicted using $1.3f'_c$. Tagawa et al. (1989) subjected a full frame to reversed cyclic loading and observed a compressive force at the column face of $1.8f'_c$. All of these specimens were fully composite with respect to gravity load provisions of the AISC LRFD specification.

A bare steel and two "partially" composite specimens were tested and reported by Leon et al. (1998) and Hajjar et al. (1998). Partially composite specimens have some shear transfer, but less shear studs than required for fully composite action for gravity load. Specimens are typically identified by the percentage of fully composite capacity provided. Specimens were reported as 35 and 55% composite. However, this was "quantified as the strength provided by the shear studs divided by the tensile strength of the steel girder" despite the fact that "the fully composite failure mode was governed by crushing of the concrete slab, not tensile yielding of the steel girder" (Leon et al. 1998, p. 870). The percentages reported would correspond to a higher percentage of composite action, if based on the critical slab capacity. At similar column tip displacements, it was found that composite specimens experienced higher strains at the bottom flanges and significantly decreased top flange distortions and strains. It was noted that the increased strains in the bottom flanges "may occur partially because the stiffer composite specimens may be more likely to rotate inelastically at a given level of interstory drift" (Hajjar et al. 1998, p. 881). In other words, increases in strain were reported for similar story drift and would not necessarily occur under similar applied moments.

Existing buildings often include a partially composite slab. An understanding of their influence on connection behavior is important when estimating the performance of retrofit or new construction SMRFs. The study results provide insight into this behavior.

This testing program was part of a larger research program on retrofit of existing steel moment connections coordinated by the National Institute of Standards and Technology. Details of the complete program can be found in Gross et al. (1999). As part of this larger, coordinated program, additional tests were conducted at the University of California at San Diego. Details of these tests are reported by Uang et al. (1998).

EXPERIMENTAL TEST SETUP AND SLAB DETAILS

Tests were performed on full-sized interior joint subassemblages loaded in a test frame, as seen in Fig. 1. The specimens were loaded at the column tip under quasi-static cyclic loading as per ATC-24 guidelines (ATC 1992). Displacement controlled load cycles of 10, 20, 30, 60, 90, 120, 150, and 180 mm (0.4, 0.8, 1.2, 2.4, 3.6, 4.8, 6.0, 7.2, and 8.4 in.) were applied. The test specimens were chosen to be representative

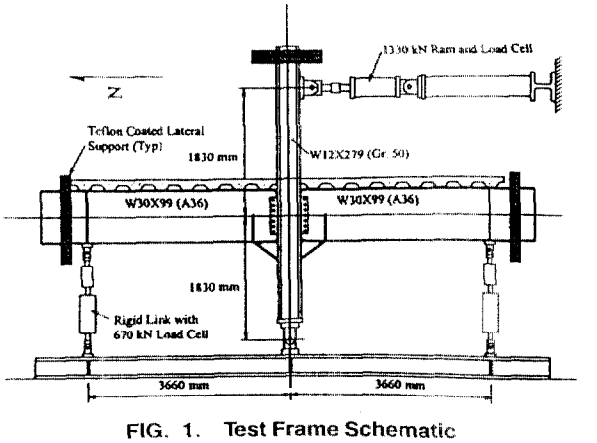

FIG. 1. Test Frame Schematic

[1]Asst. Prof., Dept. of Civ. and Envir. Engrg., Univ. of Massachusetts at Amherst, 139 Marston Hall, Box 35205, Amherst, MA 01003-5205.

[2]Assoc. Prof., Dept. of Civ. Engrg., Phil M. Ferguson Struct. Engrg. Lab., Univ. of Texas at Austin, 10100 Burnet Rd., Build. 177, Austin, TX 78758.

[3]Struct. Div., Nat. Inst. of Standards and Technol., 100 Bureau Dr., Stop 8611, Gaithersburg, MD 20899-8611.

Note. Associate Editor: Amir Mirmiran. Discussion open until August 1, 2001. To extend the closing date one month, a written request must be filed with the ASCE Manager of Journals. The manuscript for this paper was submitted for review and possible publication on November 8, 1999; revised May 31, 2000. This paper is part of the *Journal of Structural Engineering*, Vol. 127, No. 3, March, 2001. ©ASCE, ISSN 0733-9445/01/0003-0230–0237/$8.00 + $.50 per page. Paper No. 22131.

of typical building construction in common use prior to the Northridge Earthquake. Beams were W30 × 99 sections of A36 steel, typical for a large building. Columns were W12 × 279 sections of A572 Grade 50 steel to provide strong column, weak beam action and to provide for a strong panel zone. Three pairs of specimens were tested. Each pair consisted of a bare steel specimen and a similar specimen with a composite slab attached. In the first pair, the dogbone retrofit was investigated (DB1 bare steel and DB2 composite). In the second and third pairs, a haunch retrofit with differing weld procedures was investigated (HCH1 and HCH3 bare steel, HCH2 and HCH4 composite). Additional information can be found in Civjan et al. (2000).

A 2440 mm (96 in.) composite slab was included on one of the two "matched" specimens in each pair. Details were intended to be representative of typical West Coast construction practice and based on discussions with practicing engineers. The ability of a composite slab to prevent top flange weld failures was a key issue in this study. It was not the purpose of this study to find a level of slab reinforcing that would prevent top weld fractures, but merely to provide a "minimal" slab, and see if any benefit was incurred from its presence. Detailing was in accordance with this goal.

Metal decking was oriented across the beam (flutes running perpendicular to the beams). Lightweight concrete was used, and the composite action was achieved through the use of 19 mm (3/4 in.) by 140 mm (5-1/2 in.) shear studs welded at 300 mm (12 in.) on center (one stud per metal floor deck rib). Shear studs were designed to provide the capacity of the expected maximum compressive force in the concrete slab, which was estimated to be $1.3f_c$ times the effective slab area in contact with the column flange. These shear studs provided approximately 25% fully composite action under gravity load as defined by the AISC LRFD code, if the full slab width was considered effective. This ratio was 25 to 35%, if the AISC recommended effective width equal to one-eighth of the beam span were used. Shear studs were fillet welded to the beam flange using shielded metal arc welding with E7018 electrodes. A sample of these welds was then tested by bending the shear studs over 30° by use of the pipe method, in accordance with AWS D1.1-96 (AWS 1996). After most of the shear studs failed during the testing of specimen HCH2, every shear stud weld was tested in the remaining two slab specimens (HCH4 and DB2).

The No. 3 reinforcing bars were placed perpendicular to the beams to prevent longitudinal temperature and shrinkage cracking, and a 6 × 6 welded wire mesh was provided. This wire mesh provided the only longitudinal reinforcement in the slab (with the exception of two number three bars running along the perimeter of the slab). These number three bars were provided to prevent wide cracks that occurred at the slab edge in testing by other researchers (Uang et al. 1998). This cracking was felt to be unrealistic, as cracks would be somewhat limited by the continuity of the slab in a building. The number three bars were, therefore, added to provide a realistic boundary condition at the slab edges. Details of the slab are shown in Fig. 2.

The slabs were fitted with two types of gauges. Displacement transducers were provided at three locations along the length of the north beam to measure slip of the slab with respect to the beam top flange. These were located at the north end of the slab, and at the first and second metal decking flutes from the column face. In addition, points were epoxied to the slab surface at 50 mm (2 in.) gauge lengths (locations shown in Fig. 3), and deflections were measured between these points with a mechanical clip gauge (Dmec) at peak column-tip displacements. Additional points were placed on specimen HCH4 to get a better representation of compression strains at the column face. In addition, masking tape was placed at each flute of the decking to allow a visual inspection of the slip of the slab relative to the top beam flange.

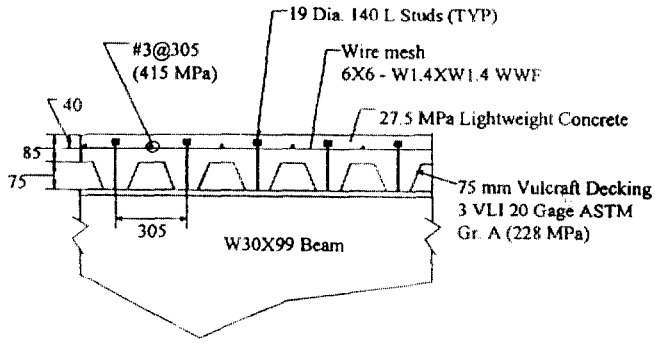

FIG. 2. Slab Details—Section View

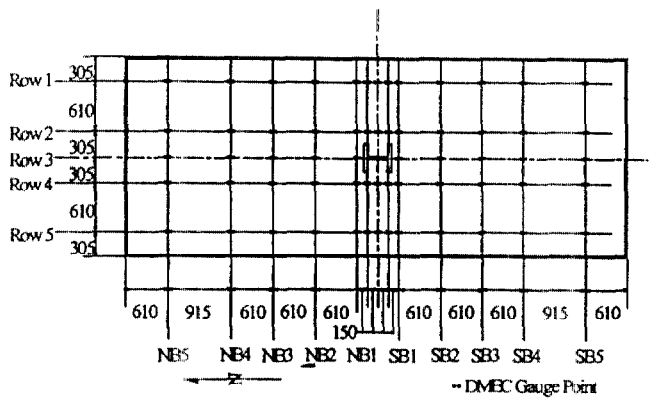

FIG. 3. Location of Dmec Gauges

ANALYSIS OF SPECIMEN "EXPECTED STRENGTHS"

Expected plastic flexural strengths (M_{ecr}) were computed for the beams of each specimen and then compared to the actual maximum moment attained in each beam during testing (M_a) (Table 1). The purpose of this comparison was to evaluate how accurately beam strength, both with and without a slab, can be estimated using simple plastic cross section analysis. The designs of the dogbone and haunch retrofits provide a "fuse" at the critical section of the beam, which limits the maximum moment at the face of the column. The critical sections are

TABLE 1. Estimated and Attained Moment Capacities

	AT CRITICAL SECTION					
	Estimated M_{ecr} (kN-m)		Attained M_a (kN-m)			
Specimen (1)	M− (2)	M+ (3)	North beam M− (4)	North beam M+ (5)	South beam M− (6)	South beam M+ (7)
DB1	1,400	1,400	1,430	1,370	1,250	1,360
DB2	1,400	1,820	1,360	1,690	1,430	1,680
HCH1	1,670	1,670	1,830	1,840	1,730	1,800
HCH2	1,670	2,290 (2,100)	1,920	2,150	2,030	2,280
HCH3	1,730	1,730	1,810	1,810	1,810	1,820
HCH4	1,710	2,060 (1,940)	2,030	2,230	1,820	2,000

Notes: Composite values based on $1.3f_c$ slab compressive stress over column face. Numbers in parentheses correspond to value of $0.85f_c$ slab compressive stress acting over column face. Critical section is center of dogbone or end of haunch location.

taken at the center of the dogbone or at the end of the haunch. The critical sections represent the weakest point along the beam relative to the moment diagram.

The expected flexural strength at the critical section of each specimen (M_{cr}) was computed using simple plastic analysis of the cross sections. These analyses assumed that all steel was at a stress of F_y and concrete in compression was at a stress of $1.3f_c'$ with an effective concrete slab width equal to the width of the column face (Du Plessis and Daniels 1972). Values of the yield stress F_y were based on actual measured values from tensile coupons taken from the specimens. The values of f_c' were based on measured concrete compressive strengths from standard cylinders tested on the same day that the specimens were tested [33.7, 42.3, and 22.2 MPa (4.88, 6.13, and 3.22 ksi)] for Specimens DB2, HCH2, and HCH4, respectively. The plastic cross-sectional analysis neglected strain hardening and concrete in tension. Further, the welded wire mesh reinforcing was also neglected in this analysis, as the area of reinforcement was quite small.

EXPERIMENTAL RESULTS

The composite specimens achieved greater plastic rotations than their bare steel counterparts, which generally failed by fracture of the beam flange groove welds. Specimens DB1 and DB2 failed by early bottom weld fractures; HCH1 and HCH3 failed by top flange weld fractures in 3 of 4 beams; and HCH2 and HCH4 deteriorated gradually due to local and lateral buckling of the beams. Details of overall behaviors are discussed in Civjan et al. (2000).

Shear Stud Failures

During testing of the composite specimens, failure of the shear studs at their welds often occurred. Locations of failed shear studs were determined through visual inspection following removal of the concrete slab after each specimen was tested. With the exception of the end shear studs, which spalled the end of the slab in all cases, all shear studs eventually failed in specimen HCH4, while in HCH2 only the second shear stud from the column face on the north beam was intact at the end of testing. Specimen DB2 did not reach the higher loads of the haunch specimens, and the shear studs were left mostly intact (four failed in the north beam, one in the south beam). The failed shear studs in DB2 were still attached to the beam flange after demolition of the concrete slab, but were easily removed from the flange by impacting the stud with a sledgehammer. Typically, shear stud welds served (Fig. 4), although at least one shear stud sheared completely through the stud itself. These failures indicated that the shear stud/weld interface (which coincides with the point of slip of the slab with respect to the beam) was the weakest link during cyclic behavior. The assumed slab compressive force, $1.3f_c'$, was not generally attained prior to the shear stud failures.

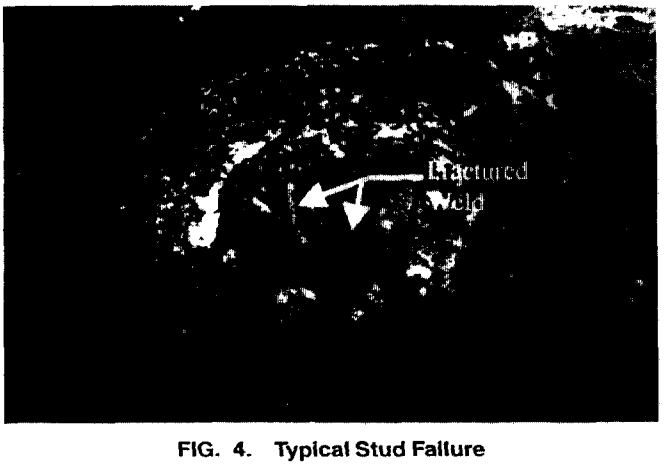

FIG. 4. Typical Stud Failure

Failures of shear studs appeared to initiate in the 60 mm (2.4 in.) load cycles, and continue through the 150 mm (6.0 in.) cycles. Failure of the shear studs was indicated by a loud bang at stages of loading for which no visible deterioration of the specimen was noted. Initially, these occurred sporadically and then in quick succession at later loadings. At the end of testing, the number of such aural indicators appeared to match the number of failed shear studs.

It is possible that transverse shear forces were present on the shear studs. A noticeable twist of the column occurred during later load cycles. Column twist was restrained by lateral support at the column tip, but only after an initial twist occurred to close the gap between the column flanges and lateral support beam [2 to 6 mm (1/16 to 1/4 in.)]. In an unrestrained specimen, this small twist at the column would cause lateral displacements at the ends of the beams on the order of 25 to 100 mm (1 to 4 in.). This twist was restrained in the steel beams by the lateral bracing at the supports. However, the slab would only be restrained against this twist by the beams through the shear studs, which could result in large transverse stresses on shear studs at the ends of the slab. Therefore, it was speculated that the shear studs may have fractured at the ends of the slab first, with fractures progressing toward the column. This observation was consistent with observations on the slip of the slab. These possible transverse shear forces would not be a realistic behavior in buildings, because the slab rotation would be resisted by the entire story's columns due to continuity of the slab.

Shear stud failures may have been due to inadequate shear stud to beam flange weld quality, shear stud capacities less than design values, or other forces on the studs. It was not possible to identify conclusively the cause of shear stud failures in the specimens. The loss of composite connection through the testing of the specimens made the slab influence at later cycles of loading much more difficult to evaluate. Shear stud failures, similar to these, do not appear to be cited in the literature on previous testing of composite sections. However, results from more recent cyclic testing of composite specimens also reported extensive failure of shear studs (Engelhardt and Venti 1999; Fry 1999). For these tests, stud welding rather than fillet welding was used. Research is currently underway at the University of Massachusetts to study shear stud strengths in more detail.

Specimen Strength

Maximum moments attained (M_a) in the beams of each test specimen are compared to the computed plastic flexural strength (M_{cr}) for each beam of each specimen in Table 1, with percentages of attained values shown in Table 2. These values are located at the critical section of each specimen, which was taken at the center of the dogbone or at the end of the haunch, as noted previously.

Both the north and south beams of the composite dogbone specimen developed positive moments on the order of 20 to 35% larger than in the bare steel specimen. Both beams of the bare steel and composite dogbone specimens ultimately failed under positive moment by fracture of the beam bottom flange groove welds. The composite specimen developed larger plastic rotations and larger moments as compared to the bare steel specimen, suggesting a potentially beneficial effect of the slab. However, the composite dogbone specimen was constructed using higher toughness weld metal as compared with the bare steel dogbone specimen. Thus, the actual influence of the slab is somewhat difficult to discern.

Examining the bare steel haunch specimens (HCH1 and

TABLE 2. Ratio of Attained Strength to Estimated Plastic Moment Capacities

Specimen (1)	AT CRITICAL SECTION			
	North Beam		South Beam	
	M− (2)	M+ (3)	M− (4)	M+ (5)
DB1	1.026	0.978	0.897	0.970
DB2	0.970	0.931	1.026	0.925
HCH1	1.096	1.103	1.035	1.076
HCH2	1.150	0.938 (1.022)	1.218	0.997 (1.054)
HCH3	1.047	1.047	1.047	1.054
HCH4	1.192	1.080 (1.145)	1.066	0.970 (1.029)

Notes: Composite values based on $1.3f_c'$ slab compressive stress over column face. Numbers in parentheses correspond to value of $0.85f_c'$ slab compressive stress acting over column face. Critical section is center of dogbone or end of haunch location.

HCH3), the data in Table 2 indicate that the beams of these specimens attained moments on the order of 1.04 to 1.10 times the computed plastic strengths. Ratios greater than 1.0 likely reflect the influence of strain hardening.

The composite haunch specimens (HCH2 and HCH4) developed larger moments than their bare steel counterparts, for both positive and negative moments. For negative moment, the composite specimens developed moments that ranged from 1 to 17% larger than the corresponding bare steel specimens. One possible source of this additional strength may be some tensile capacity contributed by the slab. However, at the point when peak negative moments were attained in the composite haunch specimens, the slab was generally extensively cracked in a direction transverse to the beam. The ability of the slab to contribute significant tensile capacity under these circumstances is questionable. Another possible explanation for the larger negative moments in the composite haunch specimens is the stabilizing effect of the slab on the beam. As will be discussed later, the slab delayed beam local and lateral torsional buckling. Since beam buckling generally results in strength degradation, the delayed buckling in the composite specimens may permit the development of larger moments.

The maximum attained positive moments in the composite haunch specimens were in the range of 10 to 27% larger than in the bare steel specimens. This likely reflects both the effects of composite action, as well as the stabilizing effect of the slab. The data in Table 2 show that the ratio of attained positive moments to the estimated plastic capacity of the composite haunch specimens are generally close to 1.0. The plastic capacity of the sections was computed assuming an effective concrete stress of $1.3f_c'$. However, since these specimens appear to have substantially strain hardened, as evidenced by the bare steel specimens, it appears that the computed plastic capacity of the composite section overestimated the actual plastic capacity. Thus, the data in Table 2 suggest that the assumed effective concrete stress of $1.3f_c'$ may not have been achieved in the composite haunch specimens. Additional data in Table 2 show that an effective concrete stress assumption of $0.85f_c'$ results in attained to estimated strength ratios similar to those attained in the bare steel specimens. It appears that effective concrete stresses realized in the specimens were at or below this value.

Flange Strains

It is sometimes assumed that since the presence of a composite slab will shift the neutral axis towards the slab, it will also result in lower strains in the top beam flange and larger strains in the bottom beam flange. An example illustrates this is not necessarily the case. Consider a W30 × 99 beam section of 345 MPa (50 ksi) steel and a fully effective slab with dimensions as per this study. A fully effective slab will have a strain of over 0.001 and, therefore, will be assumed to have 1.3 times 27.5 MPa (4 ksi) acting over the column width. For a given load on the section, say M_y of the bare steel section ignoring fillet areas [1,490 kN-m (13,230 kip-in.)], the top and bottom flanges of the bare steel section would experience a yield strain on the order of 0.00172. Assuming the steel to remain elastic and balancing forces, the composite specimen resisting this same moment would have its top flange strains reduced to 0.00072 mm/mm and its bottom flange strains also reduced to 0.00137 mm/mm. This bottom flange strain reduction occurs, because the distance between the major compression force (slab) and tension force (bottom flange) increases. One can calculate that the first yield of the bottom flange (strain of 0.00172 mm/mm) for the composite section will occur at approximately 1,750 kN-m (15,500 kip-in.). This indicates a capacity of 17% over the bare steel section. At the 30 mm (1.2 in.) load cycle, composite haunch specimens in this study achieved moments approximately 18% greater than the bare steel haunch specimens. For specimens tested in their elastic range, it would be expected that composite specimens would exhibit reduced flange strains at similar loads and similar bottom flange strains at equal story drifts.

The addition of a composite slab significantly reduced the top flange strains at the center of the dogbone section. At the bottom flange, the peak strain values were slightly reduced by the slab in the 30 mm (1.2 in.) load cycle In the haunch specimens, top flange strains at the end of the haunch location were reduced when the composite slab was included. This was more pronounced in specimen HCH2 that had a higher concrete compressive strength. Peak tensile strains were similar for all specimens, indicating that the slab had little influence when in tension. Strains at the bottom flange were not significantly affected.

Once yielding occurs in the flange, strains are highly variable depending on residual stresses, the order of yielding across the flange width, and other factors. Strain gauge readings confirmed that beyond the 30 mm (1.2 in.) load cycle, local post yielding strains varied substantially, and data were erratic.

While it has been speculated that the presence of a composite slab will increase stress on the bottom flange welds, in actuality, changes in weld stress will depend on the beam and slab cross sections.

Neutral Axis Location

The neutral axis of bending in the beams was estimated from strain gauge readings taken at the center of the dogbone or end of the haunch. For all specimens, it was not possible to determine the neutral axis location beyond the 60 mm (2.4 in.) load cycles as the data exhibited wide scatter. This was to be expected as this was typically the point at which visual records showed there to be local and lateral torsional buckling.

As expected, the addition of the composite slab to the section resulted in a neutral axis location for positive moment located nearer the top of the sections, as compared to the bare steel sections. There was a disparity between the positive- and negative-moment neutral axis locations due to the slab being much more effective in compression than in tension. The negative-moment neutral axis locations (slab in tension) approached those of the bare steel sections, despite the fact that attained negative moments exceeded those of the bare steel specimens. At later cycles of loading, the measured positive-moment neutral axis locations tended to decrease as the specimen reached its plastic moment capacity, suggesting a deterioration in composite action. All measured composite

neutral axis locations were well below the calculated plastic neutral axis values, indicating that the full plastic capacity of the slab and beam, (assuming $1.3f_c'$ acting over the column face), was not reached in the specimens through the range of reliable strain gauge readings.

Crack Patterns

The observed crack patterns were similar for all three composite specimens. The first crack in the slab occurred at the column face, extending across most of the slab by the 10 mm (0.4 in.) load cycle. During the 20 mm (0.8 in.) cycle, cracks appeared at approximately 1,220 mm (48 in.) from the original cracks. In the 30 mm (1.2 in.) load cycle (corresponding to the nominal M_n of the bare steel section), cracks appeared midway between the existing cracks at approximately a 610 mm (24 in.) spacing. Cracks generally formed at the minimum depth areas of the slab. In addition, a crack developed along the beam centerline (at the shear studs) from the column face and running approximately half the length of the slab. This longitudinal crack extended to nearly the length of the slab in the 120 mm (4.8 in.) load cycle. Later load cycles extended and expanded this cracking pattern. Slight crushing at the column flange faces initiated in the 90 mm (3.6 in.) load cycles. This crushing became more substantial at the 120 mm (4.8 in.) load cycles. In the 120 mm (4.8 in.) load cycles, the main cracks at the column face developed a vertical offset of up to 13 mm (0.5 in.), indicating that the wire fabric had probably severed. This crack was generally controlled at the edge of the slab by the longitudinal reinforcing. Subsequent loa cycles [beyond 120 mm (4.8 in.)] saw little crack development and a continuation of the crushing at the column flange faces and some web cracking at the edge of the slab. An overall view of the slab after testing is shown in Fig. 5, and a view of the column flange face is shown in Fig. 6. A compression zone is indicated by the predominantly longitudinal cracking, which extends from the corners of the column and gradually bounds a wider swath of the slab. This type of crack pattern was somewhat restrained by the transverse steel that was provided for shrinkage and temperature control.

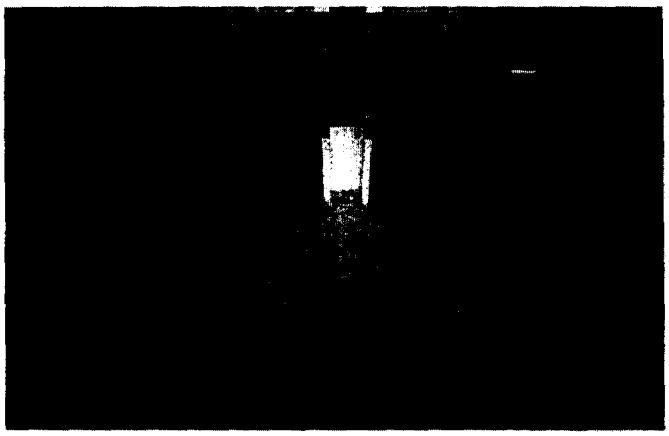

FIG. 5. Overall Cracking at End of Testing (HCH4)

FIG. 6. Cracking Pattern at Column Face (HCH4)

Slip of Composite Slab

Slippage of the slab was first visibly noticeable during the 60 mm (2.40 in.) cycles for all specimens. These were also the load cycles at which it was believed that the shear studs began to fail. Slip appeared to be constant at the end of the slab over the last 300–800 mm of HCH2 and HCH4. This length of constant peak slip progressed towards the column with subsequent loadings. This was consistent with the assumption of shear stud failures initiating at the end of the slabs and then progressing towards the column.

Slip only occurred at points where the specimen was subjected to positive moment (slab in compression). Observed slip returned to zero when the load was reversed. For the 60 mm (2.4 in.) load cycle, the slip was approximately 3 mm (1/8 in.) over a short section of constant slip at the end of the slab and tapered gradually to zero at the column face. Observed slip increased over subsequent load cycles, with a maximum value of approximately 45 mm (1.75 in.) at the end of HCH4 testing. In later load cycles of HCH2 and HCH4, the length of constant slip at the ends of the slab increased substantially over that observed at the 60 mm (2.4 in.) load cycle.

Once all the shear studs failed, the slabs began to rotate about the column centerline, presumably following the twist of the column. The slab offset, with respect to the beam flanges at the ends of the slab, was as much as 75 mm (3 in.) at the conclusion of testing. This may have played a role in the shear stud failures.

The shear studs at the column face were intact for specimen DB2 and HCH2 as indicated by the minimal slip at the first flute for the first two specimens, while HCH4 exhibited values similar to those at the second flute. Maximum second flute values reached approximately 22 mm (0.85 in.) for the 150 mm (6.0 in.) load cycles in specimens HCH2 and HCH4.

Estimate of Compressive Slab Stress

As mentioned previously, strength calculations indicated effective average concrete compressive stresses at or below $0.85f_c'$ with assumptions of concrete effective width assumed equal to the column flange width. However, the following data indicate that concrete compressive stresses at the top surface of the slab were in excess of f_c'.

Some diagonal cracks propagating from both the column flange face as well as from the inside edges of the far column flange were seen (Fig. 6). Therefore, it may be speculated that maximum concrete compressive forces may not only be increased beyond f_c', but that the effective width of the compression zone at the column face is wider than the column flange face. This increase in the effective width of the compression zone would be related to the stress distribution of the compression zone that initiates at the inside of the opposite flange face. Maximum compressive forces would be a factor of column flange width and depth. The compression zone distributed at approximately 15° to 30°, as estimated from crack patterns in the specimens.

The increased number of Dmec points at the column face of specimen HCH4 (NB1 and SB1) provided some insight into the maximum compressive forces in the slab (Fig. 7). Peak strains that would typically correlate to approximately 85% of full compression stress (about 0.0010 mm/mm) were attained

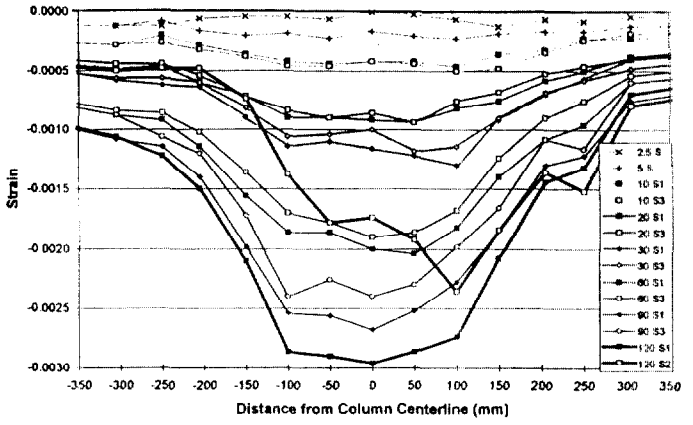

FIG. 7. Strains at Column Face (HCH4 Gauge Line SB1)

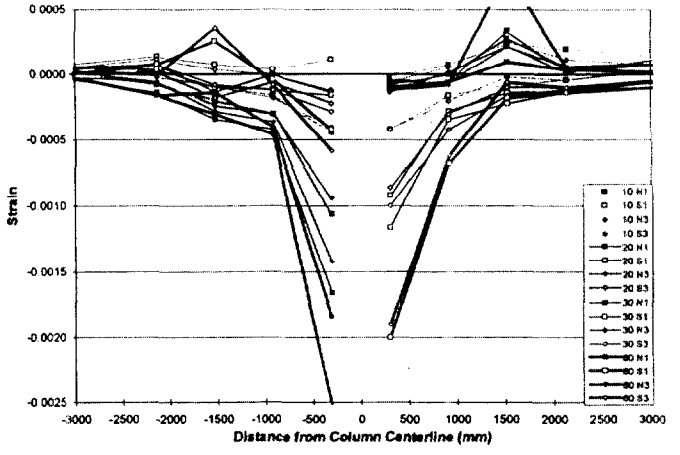

FIG. 8. Strains at Slab Centerline, Row 3 (HCH4)

for the 20 mm (0.8 in.) load cycles, while at the 60 mm (2.4 in.) load cycles, this value was exceeded across the entire 610 mm (24 in.) of gauge readings, indicating stresses on the order of f_c. The 610 mm (24 in.) width exceeds the column flange width of 330 mm (13 in.), indicating the initiation of the compression zone at the far column flange. At the 60 mm (2.4 in.) load cycles, the achieved moments were approximately 90–95% of the total achieved in the test. It was impossible to determine the actual compressive force of the slabs or estimate a strain distribution through the slab thickness due to scatter in strain gauge data at the column face.

A typical progression of strains along the column centerline (Row 3) in Dmec gauge locations, at load cycles from 10 to 60 mm (0.4 to 2.4 in.) is shown in Fig. 8. The first and third cycles had quite reproducible results through the 20 mm (0.8 in.) cycles, while the later cycles showed a loss in recorded compressive strains for the third cycle, which indicated degradation of the slab upon reloading in later load cycles. At the column faces, there was a general increase in the strains with increasing load cycles, although there was a loss in peak strain beyond the 30 mm (1.2 in.) load cycles for the later cycle at similar displacements in all specimens. This occurred even though the load held was fairly constant except in the 120 mm (4.8 in.) load cycles in which the north beam weld fractured in the second cycle of DB2. The maximum strains recorded in compression were approximately 0.0024 mm/mm for the first cycle at 120 mm (4.8 in.) of DB2, 0.0017 mm/mm for the first cycle at 90 mm (3.6 in.) in HCH2, and 0.0030 mm/mm for the first cycle at 120 mm (4.8 in.) of HCH4.

The peak strain values quickly dropped off away from the column face due to the distribution of the compressive zone across the slab. Values 910 mm (36 in.) from the column centerlines (Rows NB2 and SB2) had peak values being one-half to one-fifth those at the column face. Peak strain readings at Dmec points 305 mm (12 in.) to each side of the slab centerline (Rows 2 and 4) were approximately half the values at the centerline through the 30 mm (1.2 in.) cycles. In later load cycles, HCH4 continued this trend, DB2 saw strains increase to values on the order of the centerline values at one side of the column, and HCH2 saw similar strain increases at both sides of the column. Strains 305 mm (12 in.) from the slab edge (Rows 1 and 5) were minimal (on the order of 0.0003 mm/mm) with values depending more on the local crack configuration than the overall flow of forces. As expected, the peak slab strains occurred above the beam centerline and were maximum at the column face. It was noticed that the concrete often reached strains well above the ACI assumed rupture strains (as based on the modulus of rupture divided by the modulus of elasticity) before a crack was observed at the location.

Stability of Beam

As testing proceeded to larger deformation levels, the beams of all specimens experienced varying degrees of local flange, local web, and lateral torsional buckling. This buckling resulted in a shortening of the beams in the test specimens. Beam shortening was measured as the change in distance between the south column flange and beam stiffener above the south beam reaction. Measurements were taken at approximately 230 mm (9 in.) east and west of the beam centerline.

In an actual building, shortening of the beams would be restrained by the slab continuity and other beams and columns in the structure. Therefore, there is some question as to the validity of specimen test results where beam shortening is significant, as these restraining forces have the potential to significantly alter the behavior. Therefore care must be taken in interpreting test results at these later stages of loading. Lower observed values of beam shortening in composite specimens could indicate these specimens to be more representative of connection behavior in a structure.

For the most part, visual assessments as to the effects of the slab on beam instabilities (local and lateral buckling) were hampered by weld fractures in the bare steel specimens, beyond which extreme cases of local buckling and lateral torsional buckling were observed.

A comparative measure of instability between bare steel and composite specimens could be inferred from the beam shortening plots of Fig. 9. In comparing the beam shortening effects through the 90 mm (3.6 in.) load cycles, it was seen that all of the bare steel specimens had divergent values for the east and west sides of the beam. These differences in values from the east to west sides of the beam indicated that there was significant twist and distortions of the beam. Such behavior was still evident, but at a much smaller scale, in the composite specimens. This disparity became even more extreme at later loading cycles.

Another significant effect on local instabilities can be seen in Fig. 10. It appeared that top flange buckling was controlled by the slab. Weld failures in both bare steel haunch specimens appeared to initiate at the edge of the beam flange in contrast to the dogbone weld fractures, which appeared to initiate at the center of the welds. It is possible that if brittle fracture of welds were prevented, another source of weld fracture may be due to low cycle fatigue from high amplitude distortions. The presence of a slab appeared to control this behavior very well at the top flange. It is felt that a composite slab with metal decking placed longitudinally to the beam (or the case of a full depth slab with no metal decking) would also provide restraint to local flange buckling.

It follows that in retrofits that reduce stresses on the bottom

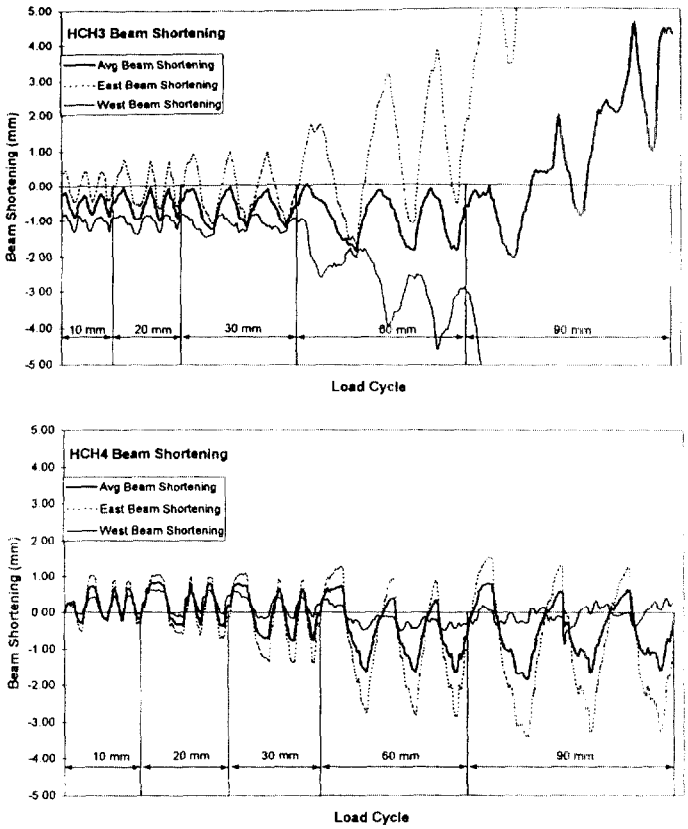

FIG. 9. Measured Beam Shortening

FIG. 10. HCH4 Buckled Shape of Top Flange (120-mm Load Cycle)

beam flange welds, such as the haunch, slab restraint to lateral torsional and local buckling may prevent later low cycle fatigue fractures at the top flange. A retrofit that has high stresses on the bottom flange (dogbone) may fracture the bottom weld at later load cycles even when weld improvements are made. Detailing for new construction (including continuity plates and high toughness electrodes) appears to provide sufficient ductility to prevent these weld fractures. In existing connections or their retrofit, however, these low-cycle fatigue fractures may become critical.

CONCLUSIONS

The influence of a composite slab on connection behavior in six full-scale subassemblages was investigated. These specimens were tested as part of a project studying the retrofit of pre-Northridge SMRF connections. Some key observations on slab effects are summarized below.

1. Composite specimens achieved greater plastic rotations than similar bare steel specimens. Top flange weld fractures occurred in the bare steel haunch specimens but did not occur in composite specimens.
2. Composite specimens exhibited a slight increase in initial elastic stiffness and strength on the order of 10 to 30% over similar bare steel specimens.
3. Composite capacities were lower than predicted, based on previous research estimates of the compressive force in the slab at the column face.
4. The slab compressive zone at the column face was found to be wider than the column face, initiating at the far column flange. The compressive strength of the concrete at the top surface of the slab appeared to be attained over this entire width at later load cycles.
5. Composite specimen top flange strains were significantly reduced from the bare steel specimens, while bottom flange strains were similar between bare steel and composite specimens. Although this may seem counter-intuitive, calculations showed this to be expected.
6. Composite specimens showed improved resistance to local and lateral instabilities of the beam sections.
7. Several shear studs failed during specimen testing. Almost all of these failures occurred at the shear stud weld. The cause of these failures is unclear and may require further study.

Beneficial effects of a composite slab include reducing the top flange stresses and delaying local and lateral torsional buckling of the beam. The presence of a composite slab did not increase the bottom flange strains for the specimens in this study.

Areas that require further research include the capacity of shear studs under reversed cyclic load and a better understanding of the effective concrete width and stress at beam-to-column connections.

ACKNOWLEDGMENTS

Primary sponsorship of this research was provided by a grant from the National Institute of Standards and Technology. The research was co-sponsored by the Northridge Steel Industry Research Fund. In addition, the Structural Shape Producers Council donated the structural steel used for the construction of test specimens. The writers gratefully acknowledge the support of these organizations.

APPENDIX. REFERENCES

American Institute of Steel Construction (AISC). (1994). *Manual of steel construction load and resistance factor design*, 2nd Ed., Chicago.

American Welding Society (AWS). (1996). *AWS D1.1-96: Structural welding code—steel*, Miami.

Applied Technology Council (ATC). (1992). *ATC-24: Guidelines for seismic testing of components of steel structures*, Redwood, Calif.

Civjan, S. A., Engelhardt, M. D., and Gross, J. L. (2000). "Retrofit of pre-Northridge moment-resisting connections." *J. Struct. Engrg.*, ASCE, 126(4), 445–452.

Du Plessis, D. P., and Daniels, J. H. (1972). "Strength of composite beam to column connections." *Rep. No. 374.3*, Fritz Engineering Lab., Lehigh University, Bethlehem, Pa.

Engelhardt, M. D., and Venti, M. (1999). "Unpublished preliminary test reports for SAC phase 2 tests." University of Texas at Austin, Austin, Tex.

Fry, G. (1999). Unpublished preliminary test reports for SAC phase 2 tests, Texas A&M University, College Station, Tex.

Gross, J. L., Engelhardt, M. D., Uang, C. M., Kasai, K., and Iwankiw, N. R. (1999). "Modification of existing welded steel moment frame connections for seismic resistance." *Steel Design Guide Series, No. 12*, American Institute of Steel Construction, Chicago.

Hajjar, J. F., Leon, R. T., Gustafson, M. A., and Shield, C. K. (1998). "Seismic response of composite moment-resisting connections. II: Behavior." *J. Struct. Engrg.*, ASCE, 124(8), 877–885.

Lee, S. J., and Lu, L. W. (1989). "Cyclic tests of full-scale composite joint subassemblages." *J. Struct. Engrg.*, ASCE, 115(8), 1977–1998.

Leon, R. T., Hajjar, J. F., and Gustafson, M. A. (1998). "Seismic response of composite moment-resisting connections. I: Performance." *J. Struct. Engrg.*, ASCE, 124(8), 868–876.

Strategic Air Command. (SAC) Joint Venture. (1995). "Interim guidelines: Evaluation, repair, modification, and design of welded steel moment frame structures." *Report No. FEMA 267*, Federal Emergency Management Agency, Washington, D.C.

Tagawa, Y., Kato, B., and Aoki, H. (1989). "Behavior of composite beams in steel frame under hysteretic loading." *J. Struct. Engrg.*, ASCE, 115(8), 2029–2045.

Uang, C. M., Yu, Q. S., and Noel, S. (1998). "Rehabilitating pre-Northridge steel moment frame connections: RBS and haunch approaches considering slab effects." *Proc., 6th U.S. Nat. Conf. Earthquake Engrg.*, Earthquake Engineering Research Institute, San Francisco.

Youssef, N., Bonowitz, D., and Gross, J. L. (1995). "A survey of steel moment-resisting frame buildings affected by the 1994 Northridge earthquake." *NIST Rep. No. NISTIR 5625*, National Institute of Standards and Technology, U.S. Dept. of Commerce Technology Administration, Washington, D.C.